Title: Consequences of sea level rise for high metal(loid) loads in the Ría of Huelva estuary sediments

Carolin F. Kerl[1], M. Dolores Basallote[2], Merle Käberich[1], Erica Oldani[1], Nathalia P. Cerón Espejo[1], Andrea E. Colina Blanco[1], Carlos Ruiz Cánovas[2], José Miguel Nieto[2], Britta Planer-Friedrich[1]*

[1]Environmental Geochemistry, Bayreuth Center for Ecology and Environmental Research (BayCEER), University of Bayreuth, D-95440 Bayreuth, Germany

[2]Department of Earth Sciences & Research Center on Natural Resources, Health and the Environment (RENSMA), University of Huelva, Huelva, 21071 Spain

* Corresponding author phone: +49 921 55 3999, E-mail: b.planer-friedrich@uni-bayreuth.de

Highlights

- Sea level rise, can initiate long-lasting metal(loid) mobilization from a mining-impacted estuary
- Sea level rise increases cation mobilization in sediments by competitive desorption
- Mobilization during short-term seawater flooding is mainly pH-dependent
- Long-term seawater flooding will increase former acidic sediment pH to neutral pH
- Mobilization during long-term seawater flooding is salinity-dependent

Abstract

Ría of Huelva, located in southwestern Spain, is a highly metal(loid)-contaminated estuary system where sediments are exceeding action limits in an increasing order for Cd, Zn, Pb, Cu, and As. With a predicted sea level rise over the next 50 years, the estuary will be subject to flooding with brackish water or seawater. To evaluate the risk of metal(loid) mobilization under future climate scenarios, different locations along the estuary were sampled at different depths. Samples were flooded with river water, brackish water, and seawater under different short- and long-term laboratory setups. Potential metal(loid) mobilization showed that water quality standards for As, Pb, Zn, Ni, Cu, and Cd could be exceeded upon seawater flooding. However, metal(loid) mobilization was not predictable solely based on sediment loads. The driving factors for cation and anion mobility were identified to be mainly pH under low salinity and competitive desorption under high salinity conditions. Further drivers such as wave movement or labile C input in C-limited systems were found to enhance metal(loid) mobilization. Long-term flooding of intact sediment cores revealed that sea level rise will have different effects on the estuary system depending on duration of flooding. Short-term flooding in the

near future will first affect alkaline sediments and enhance currently low cation mobilization, while anion mobilization due to reductive Fe dissolution will remain high. Once acidic sediments further inland are flooded with seawater, highest contaminant mobilization can be expected as high salinity will further enhance already high cation mobilization under acidic pH. Long-term flooding with seawater will neutralize the sediment pH and limit cation mobilization compared to acidic pH. However, the contaminant load stored in the estuary is so high that, extrapolating data obtained, mobilization could last for more than 1000 years, e.g. for As, Pb, and Al.

TOC

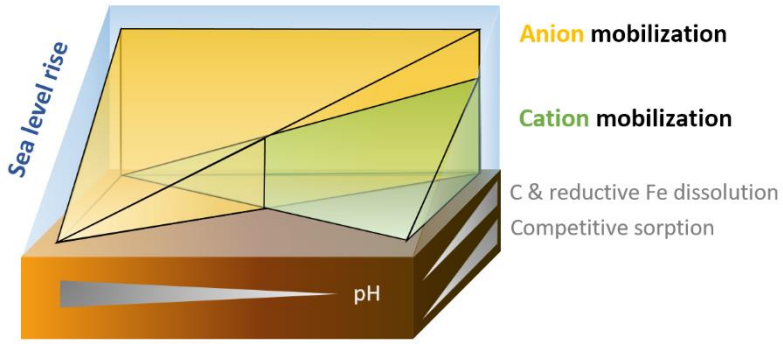

Ría of Huelva (SW Spain)

Keywords

Mining-impacted estuary, Río Tinto, Río Odiel, climate change, contaminants, metal(loid) mobilization

1 Introduction

Ría of Huelva estuary, located in southwestern Spain, is formed by the rivers Río Tinto and Río Odiel which discharge into the Atlantic Ocean near the City of Huelva. It is considered one of the most metal(loid)-polluted fluvial-estuarine systems in the World, resulting from extensive mining of massive sulfide deposits in the nearby Iberian Pyrite Belt since pre-Roman times (Davis Jr et al., 2000). Oxidation of sulfides causes formation of acid mine drainage (AMD) with release of a variety of metal(loid)s (e.g. Fe, As, Pb, Cu, Zn, Ni, Cd, Cr) (Nieto et al., 2007; Olías and Nieto, 2015). Río Tinto and Río Odiel, which drain the mining areas, are extreme AMD environments, constantly transporting metal(loid) loads of several tons per year, e.g. Río Tinto Fe 5075 t/a, As 12 t/a, Pb 15 t/a, Cu 469 t/a, and Zn 863 t/a or Río Odiel Fe 2847 t/a, As 23 t/a, Pb 12 t/a, Cu 1252 t/a, and Zn 2612 t/a. These values represent an important fraction of the global gross flux of dissolved metals (mainly Zn and Cd) transported by rivers into the ocean (Olías et al., 2006). Near the City of Huelva, discharges from industries (e.g. copper smelting, fertilizer production, or oil and gas refinery) as well as leaching from a phosphogypsum stack from a phosphate fertilizer industry further contribute to the metal(loid) load in the estuary (Pérez-López et al., 2011). Sediments of the estuary partly sequester incoming metal(loid)s, leading to excessively high sediment contents up to the g/kg range e.g. for As, Pb, Cu, Zn, but also to a very heterogeneous distribution of sediment contents (Borrego et al., 2002; Elbaz-Poulichet et al., 2001; Morillo et al., 2008). Sequestration of contaminants to the sediment is especially enhanced in the upper part of the estuary where Río Tinto and Río Odiel reach the tidal zone and the AMD mixes with alkaline sea water (SW), producing a sharp pH gradient from pH 3 to 8 within 20 to 30 km (Achterberg et al., 2003; Basallote et al., 2019; Canovas et al., 2020).

High metal(loid) concentrations impact freshwater quality, marine life and potentially human health (e.g. via contaminated seafood and freshwater fish or groundwater contamination). More and more concerns about potential adverse health effects of metal(loid) pollution are arising in recent years (Rosado et al., 2016), with Huelva province being among the areas with the highest mortality risk in Spain (Benach et al., 2004). The current situation already poses risks for humans and ecosystems, however, climate change within this century might add further risks to the estuary system, e.g. sea level rise or an increase in frequency and intensity of precipitation events leading to floods (IPCC, 2021). Despite comprehensive research about the metal(loid) pollution in the estuarine sediments, studies about possible metal(loid) mobilization by expected flooding through sea level rise are still scarce.

Climate change is predicted to increase sea levels by 16 to 61 cm (5-95% percentile) until the year 2050 compared to 2000, inundating low elevation estuaries with SW including the Ría of Huelva (Bamber et al., 2019; IPCC, 2021; Kulp and Strauss, 2019). Upon inundation by SW, sequestered metal(loid)s can be remobilized (Hutchings et al., 2019; Wong et al., 2015). Given a suitable carbon source, bacterial

dissimilatory reductive dissolution of Fe and Mn (hydr)oxides takes place releasing reduced Fe and Mn and previously bound metal(loid)s. Reductive dissolution was determined especially relevant for As mobilization (LeMonte et al., 2017), however, cationic metals (e.g. Zn, Cu, Ni) can also be mobilized by reductive dissolution of Fe and Mn (hydr)oxides (Wong et al., 2015). Additionally, competitive ion exchange increases with SW inundation compared to fresh water because higher ionic strength enhances metal(loid) desorption from sediments (Wong et al., 2015). Cations are particularly exchanged, but anionic metal(loid)s (e.g. As) may be affected, too (Johnston et al., 2010). Moreover, acidic pH increases exchange of cations by competition with protons for negatively charged sorption sites, leading to further acidification (Wong et al., 2010; Wright et al., 1988). So far, the influence of sea level rise has not been assessed in a multi-contaminated site like the Ría of Huelva estuary.

Further, the influence of tidal inundation on metal(loid) mobilization from sediments is still poorly understood. First results suggest that metal(loid) mobilization may be enhanced by tidal inundation compared to stagnant flooding since alternating redox conditions during tidal inundation enhance formation of soluble metal(loid) phases and migration of metal(loid)s towards particle surfaces. Through repeated dissolution/precipitation of minerals, the bio-accessibility of metal(loid)s bound to surfaces increases (Han et al., 2019; O'Connor et al., 2021). Although the Ría of Huelva estuary is one of the most metal(loid) polluted estuaries worldwide, there are also many other estuaries affected by AMD, like the Zuari estuary in India (Gaonkar and Matta, 2019), the Bahia de Ite in Peru (Dold et al., 2011), the King River in Australia (Koehnken, 1996) or the Fal Estuary in the UK (Pirrie et al., 2003). Insights gained at the Ría of Huelva estuary will therefore also have implications for similar sites worldwide.

To address the knowledge gaps of both effects of sea level rise in general and tidal inundation specifically, sediment cores were collected from seven sites within the Ría of Huelva estuary, predicted to be inundated in 2050. After general characterization, potential metal(loid) mobilization by sea water and brackish water was determined for the different layers of each core. Further, short-term metal(loid) mobilization was determined at one site with a low sediment pH and low C content-and at another site with a high sediment pH and high C content. For both sites, mobilization was determined for a salinity gradient from river to sea water and under the influence of physical disturbance, mimicking wave movement. For the low C-site, mobilization was also determined under enhanced C-availability. Long-term flooding (1 year) under stagnant and tidal conditions was also conducted for cores from both sites to monitor metal(loid) leaching and sediment characteristics over time.

2 Material & Methods

2.1 Study area description

Sediment samples were taken from the salt marshes of the Río Tinto and Río Odiel located in the province of Huelva (SW, Spain) along the Atlantic coast of the Gulf of Cadiz. Seven locations were chosen, five for the Río Tinto (0, A1, A2, B, and C) and two for the Río Odiel (A and B, Figure 1, Table Appendix 1).

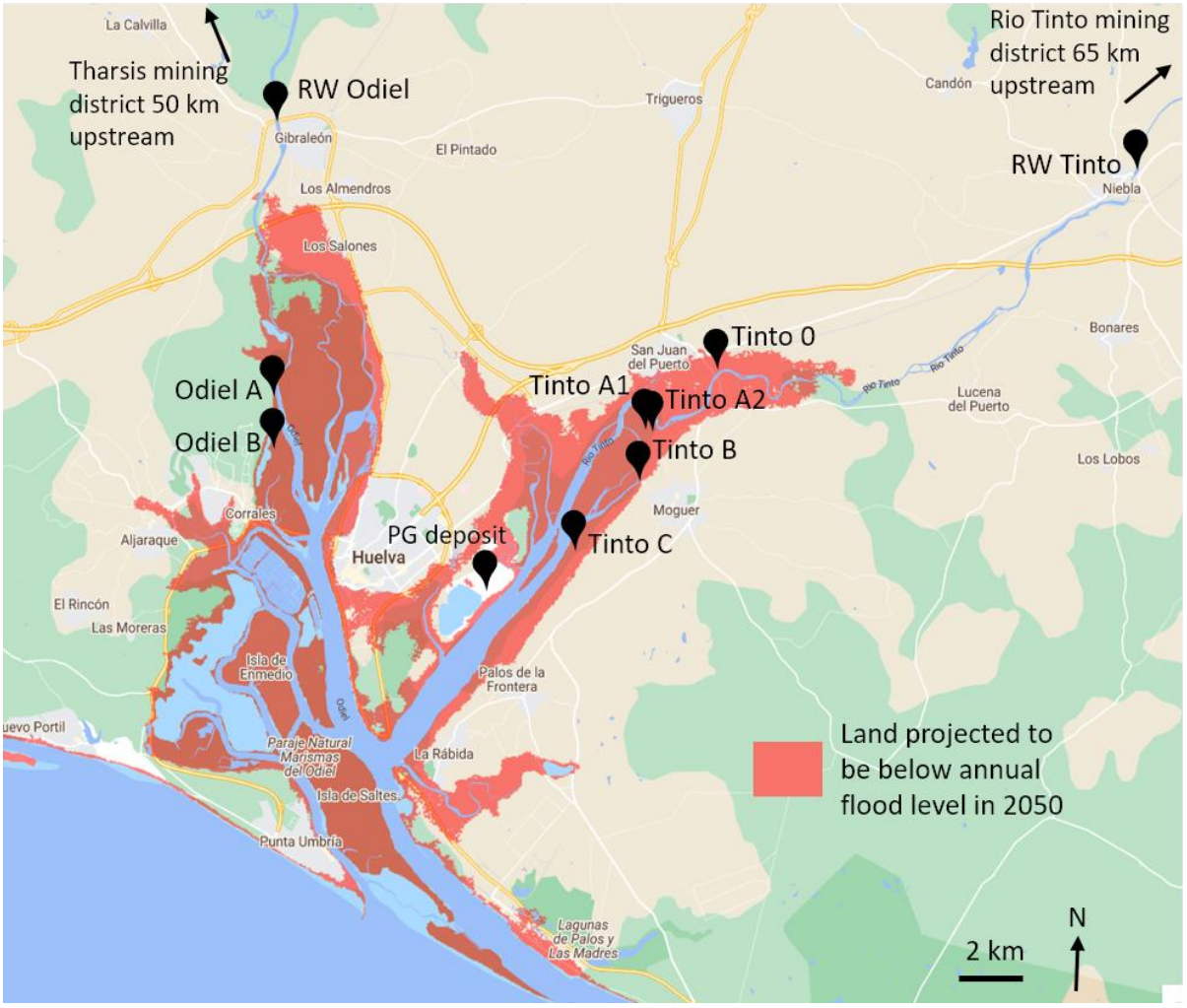

Figure 1: Map of the Ría of Huelva estuary with the location of sampling points; in red the area predicted to be inundated with sea level rise by 2050 (Kulp and Strauss, 2019); PG: location of the phosphogpysum (PG) stack near Huelva. Map downloaded from Climatecentral.org (2021) using the following keywords for the Simulation: Projection Type(sea level rise + annual flood); Sea Level Scenario (current trajectory); Luck (bad); Areas to show as threatened (exclude areas isolated by higher land); Sea-level-projection source: Leading Consensus (IPCC 2021) https://coastal.climatecentral.org/map/12/-6.8843/37.2712/?theme=sea_level_rise&map_type=year&basemap=simple&contiguous=true&elevation_model=

best_available&forecast_year=2050&pathway=ssp3rcp70&percentile=p95&refresh=true&return_level=return_level_1&rl_model=gtsr&slr_model=ipcc_2021_med .

Sampling sites were selected to compare AMD-affected sediments from both estuaries, taking high spatial heterogeneity into account and excluding input of diffuse anthropogenic pollution present in the lower estuary area. Sampling locations were downstream of San Juan del Puerto, which marks the approximate upper limit of tidal influence. The sampling sites are located 65 to 75 km and 50 km downstream of the Río Tinto and the Tharsis mining districts, respectively, and approximately 20 to 30 km upstream from the ocean.

Five locations were selected in the Río Tinto estuary zone, going north to south along its eastern channel:

- *Site Tinto 0 (T0)*: around 40 m from the river and dominated by Río Tinto freshwater
- *Sites Tinto A1 & A2 (TA1 & TA2)*: around 215 m and 50 m from the river, respectively, to compare non-flooded and periodically flooded areas. Thus, the sediment is mostly under river water influence, experiences tidal SW influence only when extreme flooding events occur, and dries up frequently.
- *Site Tinto B (TB)*: around 30 m from the river, periodically inundated by Río Tinto and exposed to a stronger tidal seawater influence.
- *Site Tinto C (TC):* around 300 m from the river with the strongest tidal influence. This point is the closest to the phosphogypsum stacks adjacent to the western border of the Río Tinto.

Río Odiel salt marshes are located approximately 3.5 km west of the Río Tinto marshes. In this area, two sampling sites were selected along the western river channel, where recent mining influence is more prominent.

- *Site Odiel A (OA):* around 20 m from the river and at comparable distance from the ocean like TA1 and TA2.
- *Site Odiel B (OB):* around 130 m from the river; at this site, pyrite ashes were dumped in the past due to mineral processing operations.

In general, the whole estuary area is characterized by high spatial-temporal heterogeneity, with small scale variations in sediment color along the sediments profiles and the redox interfaces at varying depths.

2.2 Field sampling

The first sampling took place in February 2020. Cores (30 ± 5 cm depth) were obtained by manually pushing polyvinyl chloride (PVC) tubes (60 cm in height, 5.7 cm in diameter) into the marsh ground. At

each sampling site, one intact sediment core was collected for general characterization. Cores were stored cool and dark until dissection.

River water of Río Tinto (close to Niebla, Figure 1) and Río Odiel (close to Gibraleon) were collected upstream from the estuary area, where seawater influence was assumed to be negligible. Approximately 2 L of water were collected and stored cooled and dark immediately after collection.

In April 2021 and 2022, additional bulk sediment was sampled at sampling sites TA1 and TB. From each site, the upper 5 cm of sediment were removed, and 5 kg of bulk sediment were taken from 5 to 30 cm. In April 2021, additionally 5 intact sediment cores were sampled from TA1 and TB each and Río Tinto river water (RW) was collected close to Niebla.

2.3 Core dissection and basic characterization

All samples were transported from the study area to Germany and processed within a week. Cores were sliced horizontally and then separated in sections according to visible layering along profiles (varying between 1.5 to 7 cm). Immediately after dissection, sections were flash frozen, freeze dried and manually homogenized. The following parameters were determined for all sediment layers and bulk sediment samples: sediment pH, C/N, elemental concentrations after aqua-regia digestion and sequential extraction.

2.4 Experimental setups

Potential metal(loid) mobilization was determined by mixing 6 mL synthetic SW ((ASTM, 2003), Table A2) with 2.5 g of dried, homogenized sediment from each layer under anoxic conditions inside a glovebox (Coy, 95%/5% nitrogen/hydrogen). The bottles were sealed with rubber stoppers and aluminum caps and stored in the dark at constant temperature of 21°C for 65 days (d). For the upper 15 cm of the cores, incubations with each layer were repeated with brackish water (BW) at three different SW:RW ratios (20:80%, 50:50%, 80:20%). After incubation time, sediment suspensions were separated under anoxic atmosphere by suction filtration using 0.2 µm cellulose acetate (CA; Th. Geyer) filters. For liquid samples, pH and S(−II) were determined immediately and subsamples were stabilized in 0.45% (v/v) H_2O_2 (30%, Kraft) and 0.81% (v/v) HNO_3 (65%, Kraft) for total metal(loid) analysis by ICP-MS. Solid samples of SW incubation were freeze-dried and total metal(loid) content was determined after aqua-regia extraction by ICP-MS.

Detailed experiments on factors driving short-term metal(loid) mobilization were carried out with two bulk sediments which represent two extremes within the estuary: site TA1 with low sediment pH and low C content and site TB with high sediment pH and high C content (Table A3). Of the homogenized wet bulk sediments TA1 and TB (sampled in 2021), 200 g were inundated in 1 L PE bottles for 60 d at 20 °C in darkness with RW, SW and BW (50% RW, 50% SW). Seawater was amended with 100 µM

dissolved organic carbon (DOC), a typical SW concentration (Dafner et al., 1999), in form of D(+)-Glucose (99%, Grüssing). For each inundation water, treatments with water saturation of sediments ('saturated') and 1 L of overlaying water phase ('submerged') were conducted in triplicates. Little differences were found for saturated and submerged treatments and results are summarized. Individual results can be found in Figure A14. Pore water samples were taken at day 1, 3, 5, 9, 15, 30, and 60 with rhizon samplers (Rhizon MOM 5 cm with pore size of membrane 0.12 to 0.18 µm, Rhizosphere) permanently installed in the sediments. Until stabilization or analysis, samples were handled anoxically. Redox potential, pH, and electrical conductivity (EC) were measured in pore water samples, Fe(II), total Fe, S(−II) were determined photometrically, and total metal(loid) contents were measured by ICP-MS after stabilization in 0.45% (v/v) H_2O_2 and 0.81% (v/v) HNO_3.

The experiment was repeated in 2022 for TA1 sediments under enhanced C influence. Therefore, sediment was amended with 0.01, 0.1, and 1% C as D(+)-Glucose and inundated only with SW under submerged conditions. High pulses of labile C where chosen to mimic scenarios such as algae blooms, storms and floods with overflowing waste water treatment plants, oil spills, or manure drainage from agricultural and livestock farms.

The influence of waves on metal(loid) mobilization was simulated by shaking (Varioshake VS 8 BE, Lauda at 125 rpm) an equivalent of 4 g dry weight of bulk sediments TA1 and TB under oxic conditions with 10 mL and 100 mL SW in triplicates. Samples were taken after 48 h, filtered (0.20 µm CA, Macherey-Nagel), and analyzed for total metal(loid) content after stabilization in 0.45% (v/v) H_2O_2 and 0.81% (v/v) HNO_3.

Long-term metal(loid) mobilization under realistic natural conditions was simulated by stagnant and tidal inundation with SW of sediment cores for 1 year. Five cores were sampled in April 2021 from site TA1 and TB. One core was used for characterization of original conditions and 4 were exposed to stagnant and tidal inundation with SW at 20 °C in darkness. For stagnant inundation, two cores of each sediment were flooded with 500 mL SW. For tidal inundation, 500 mL SW were pumped on and off the cores in a tidal rhythm (6 h high tide, 6 h low tide), resulting in a SW flow rate of 1.4 mL/min. A 10 L SW reservoir was used per sampling site for tidal inundation and occasionally refilled. The exposed cores were sampled after 100 and 365 d and dissected as described previously. Sediment pH, total metal(loid) content, and amorphous and crystalline Fe(III) were determined in freeze-dried and homogenized layers.

2.5 Solid phase analysis

Sediment pH was determined by shaking 2 g of freeze-dried, homogenized sediment with 5 mL 0.01 M $CaCl_2$ (99.5%, Grüssing) for 30 min on an overhead shaker (Model 3040, GFL) at 20 rpm. Samples were centrifuged for 10 min at 3500 rpm (Rotofix 32 A, Hettich) and pH was measured in the supernatant.

Total sediment carbon and nitrogen contents were determined with a CHN elemental analyzer (Thermo Quest, Flash EA, 1112).

To determine total metal(loid) contents, sediment layers were extracted by microwave digestion (MARS Xpress, CEM) in aqua regia (HCl 32 % + HNO3 65 %, ratio 3:1, 20 min heating to 160°C, 15 min holding the temperature). Extracts were filtered (0.20 µm CA) and analyzed by ICP-MS. The procedure for the sequential extraction is described in Table A4.

Amorphous Fe was determined using ammonia oxalate extraction, by adding 10 mL 0.2 M ammonia oxalate ($C_2H_{10}N_2O_5$, 99.5%, Grüssing; pH 3.25) to 0.4 g of freeze-dried, homogenized sediment. Reaction vials were shaken for 4 hours at 200 rpm and centrifuged at 3500 rpm for 15 min. The sediment was washed with 5 mL of 0.2 M ammonia oxalate (pH 3.3) for 10 min, centrifuged and supernatants were combined to measure total Fe photometrically.

Amorphous and crystalline Fe were extracted from sediments by dithionite-citrate-bicarbonate (DCB) extraction according to Mehra (1960). Briefly, 8 mL 0.3 M sodium citrate ($C_6H_5Na_3O_7 \cdot H_2O$, 99%, Sigma-Aldrich) and 1 mL 1 M sodium bicarbonate ($NaHCO_3$, 99.5%, Grüssing) were added to 0.4 g of freeze-dried, homogenized sediment. Reaction vials were heated to 80 °C in a water bath and held at this temperature for 30 min. Approximately 0.2 g sodium dithionite ($Na_2O_4S_2$, 85%, Sigma-Aldrich) were added and samples were reintroduced to the water bath for 15 min before centrifugation at 3500 rpm for 15 min. Total Fe was measured photometrically in supernatants. Crystalline Fe was determined by subtracting the amount of amorphous Fe determined by ammonium oxalate extraction.

2.6 Liquid phase analysis

Redox potential and pH (HQ40d with MTC101, PHC101, Hach), as well as EC (WinLab, Windaus Labortechnik with LCV 0.35/21, Meinsberger Elektroden) were measured. Redox potential was converted to EH values and then to electron activity (pe). Redox conditions were classified as oxic (pH+ pH >14), suboxic (9-14), or anoxic (<9) (Blume et al., 2016; Fiedler et al., 2007). Fe(II) and total Fe concentrations were analyzed by the ferrozine method (Stookey, 1970) at 570 nm with a microplate reader (Infinite 200Pro, Tecan). For S(−II) in pore water, the methylene blue method (Cline, 1969) was used, measuring at 650 nm.

2.7 Total metal(loid) contents

Total contents were measured by ICP-MS (X-Series 2, Thermo Scientific and 8900 ICP-MS Triple Quad, Agilent). Detailed information about measurements can be found in Table A5. Certified reference materials (TMDA 54.5 or TMDA-62.2, Environment Canada) were used to check quality of

measurements. Internal standards (Rh [Rh^+, m/z 103] and Re [Re^+, m/z 187]) were applied to compensate for signal drift.

2.8 Statistical methods for data processing

Correlations and principal component analyses (PCA) were calculated using the R and RStudio software (R Development Core Team, 2008). Pearson correlation coefficients were used to assess the significance of all correlations presented.

3 Results & Discussion

3.1 Metal(loid) load in Río Tinto and Río Odiel estuary

Sediment metal(loid) contents showed a large spatial heterogeneity among the seven sampled cores (Figure 1, A1,A2) due to differences in deposition history in the braided river systems, seasonal flooding, tidal influence and additional anthropogenic input. Sediment pH increased with increasing SW influence towards the coast (pH 3.6 to 7.4 in the upper layers of T0 to TC, respectively; Figure A1, Table A6) while sediment C distribution did not show an overall trend towards the coast. However, Tinto cores (0.6-3.6%), especially site TB, have higher C contents than Odiel cores (0.3-1.1%).

Decision tree (Figure A3), PCA (Figure A4), and correlation analyses (Appendix B) showed that contaminant loads in the estuary cannot be predicted based on simple general parameters such as pH, C, Fe, S, P, Mn, Al, or sediment color because of the sediments´ large heterogeneity. However, across all cores, Fe, S, As, Sb, Pb as well as C, Cd, Cu, Zn and P, U showed similar trend (Figure 2a, A5, A6). High concentrations of Fe- and S-associated contaminants were found at low sediment pH (<4, e.g. T0) as expected for anions like As and Sb, but also for Pb (Figure 2b-d). Even though a cation, Pb is sorbed to Fe-minerals as low as pH 3 (Fischer et al., 2007). This may be related to the precipitation of Fe and Al oxyhydroxysulfates during estuarine mixing processes at pH values below 5 (Asta et al., 2015). Contaminants associated with C (Cu, Cd, and Zn), were enriched at high pH (>6, e.g. TB & TC) as expected for these cations (Figure 2e-g). Elements with a high affinity to C such as Cd, Cu, and U showed a clear trend towards accumulation with high C content especially in TB. Phosphorus associated U and also Cd (Figure 2i & h), more prominent in TB & TC, most likely do not originate from the mining area, but are leached from the phosphogypsum stack close to site TC (Figure 1) (Borrego et al., 2002).

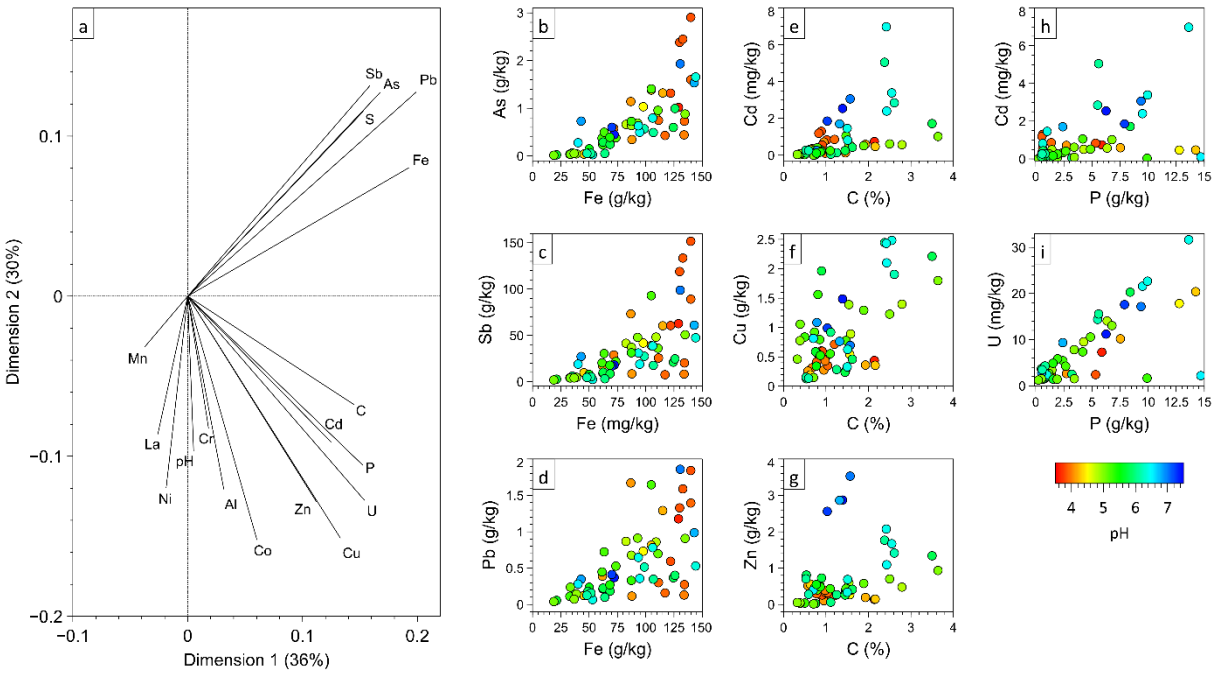

Figure 2a: PCA using pH and elemental content in all sediments layers of all cores as parameters. Data were normalized to largest values. 2b-i: Metal(loid) content of sediment layers against sediment Fe and C content, as well as U against P sediment contents. Sediment pH is reflected by color of data points.

For evaluating the risk of metal(loid) mobilization under future climate scenarios, the current contamination load was evaluated by comparing obtained data to action levels (AL; below AL1: disposal permitted, between AL1 & AL2: further studies required prior to disposal, above AL2: material must be isolated, above 8*AL2: special isolation techniques are required) for disposal of dredged sediments and ERM (effects range-median) above which biological effects are expected frequently (Figure 3, Table A7 (DelValls et al., 2004; Long et al., 1995)). Measured Ni and Cr concentrations were below thresholds, while all Cd values were below the ERM, but site TB and upper TC were above AL1. The situation for Zn was more heterogeneous as most sites were below AL1, whereas sites TA2, TB, and TC were between AL1 and AL2. Overall 52% of sampled layers were above the ERM. Lead values showed a wide concentration range; however, all values in the upper layers exceeded AL1. Especially high concentrations were observed at sites T0 to TB, where upper layers exceeded AL2 by up to 3-fold and 82% of all layers sampled at Río Tinto sites exceeded the ERM compared to only 40% at Río Odiel sites. For Cu, all samples exceeded AL1 and all upper layers were above AL2 by up to 6 times. More than 90% of samples exceeded the ERM in Río Tinto and more than 70% in Río Odiel estuary. The severest contamination was found for As, where all upper layers were above AL2 and ERM. At site T0, the first 17 cm were up to 14-times above the AL2 and are therefore classified according to the highest contamination category (>8*AL2). The As contamination was more pronounced in Río Tinto estuary

where more than 90% of the samples exceeded the ERM compared to only 33% in the Río Odiel estuary. Similar metal(loid) concentration were reported in the estuary before (Borrego et al., 2002). The site characterization showed that Río Tinto estuary generally has even higher metal(loid) loads for Fe, Cu, Zn, As, Cd, Sb, Pb, and U than Río Odiel. However, both estuaries are highly heterogeneous in their metal(loid) loads. Especially high loads of the potentially toxic elements Zn, Pb, Cu, and As, stored in sediments, could pose a risk for further mobilization under changing hydrological regimes.

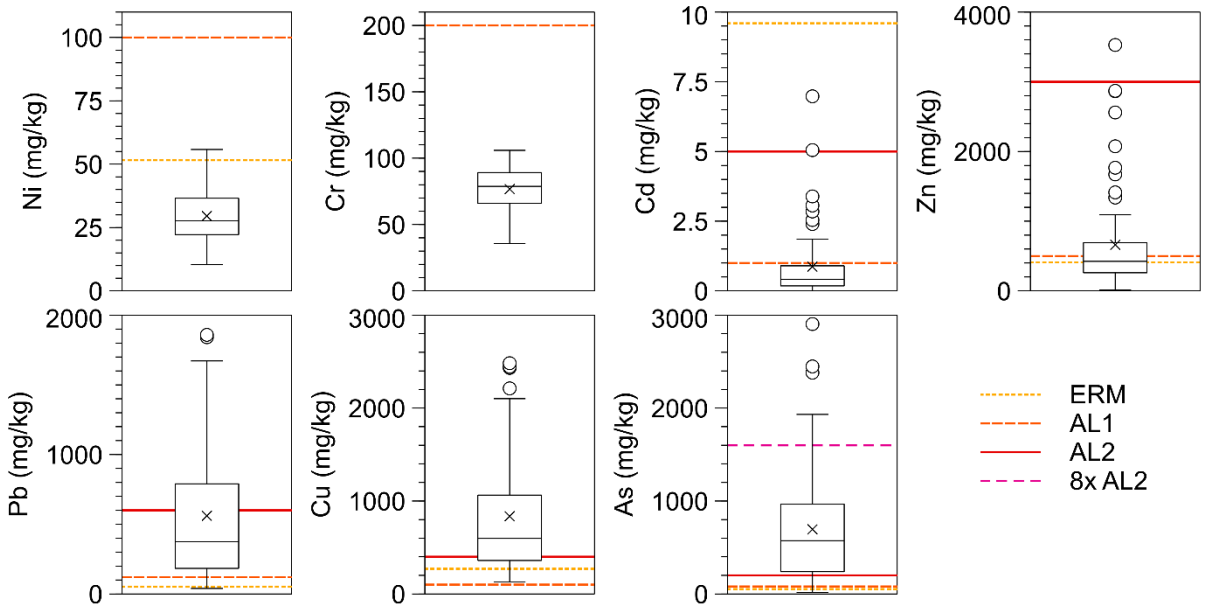

Figure 3: Boxplots of metal(loid) content in sediment all layers of all cores. Action levels (AL; below AL1: disposal permitted, between AL1 & AL2: further studies required prior to disposal, above AL2: material must be isolated, above 8*AL2: special isolation techniques are required) for disposal of dredged sediments and ERM (effects range-median) concentrations are shown according to Spanish legislation (DelValls et al., 2004; Long et al., 1995). Box plots: line, median; cross, mean; box, interquartile range; whiskers, 1.5 interquartile range.

3.2 Potential metal(loid) mobilization from sediment layers

To evaluate the metal(loid) mobilization potential of the estuary system, all layers of the 7 cores were incubated anoxically with SW. Mobilization after 65 d was as heterogeneous as the metal(loid) reservoir in the sediment cores (Figure A7, A8). Due to the complex system (varying pH, C, Fe, Al, Mn contents), no parameter was found that could predict metal(loid) mobilization in the estuary based on sediment loads (Appendix C). Sequential extractions of sediments performed to identify easily extractable fractions of metal(loid)s, could not predict mobilization either because high ionic strength of SW was not mimicked (Table A4, Appendix D).

In relation to the large reservoir of metal(loid)s in the estuary, overall mobilization to SW was mostly below 1%, except for Mn, Co, Cu, Zn where mobilization of up to 12% occurred in single layers. Exceptionally high Cd mobilization was found at both Odiel sites with up to 89% (Figure A9), which could be attributed to the different retention mechanisms within the sediment. Thus, Cd may be sorbed onto Fe and Al minerals in the Odiel sediments, while in the Tinto may be hosted by carbonates. However, even relatively low mobilization compared to the sediment reservoir can lead to elevated metal(loid) concentrations in the overlaying water. Taking Spanish national environmental quality standards for surface water into account (Table A8), 73-98% of all samples exceeded the limits for Cd, Cu, Ni, and Zn in the estuary (BOE, 2015). For Pb 42% and for As only 27% of all samples were above water quality standards, even though As was the element exceeding sediment quality standards the most. These results clearly show that simply surveying contaminant loads in the estuary is not enough to predict further metal(loid) mobilization and additional geochemical factors need to be taken into account as shown before e.g. (Allen, 1993; Atkinson et al., 2007). Correlation analyses showed that C and sediment pH were the parameters most helpful in estimating mobilization of contaminants (Figure 4a-g, A10 & A11, Appendix B & C). The anions As (pH>6) as well as V and U (both pH>7) clearly showed increasing mobility with increasing pH (Figure 4a-c), whereas lower mobility was found for the cations Al (pH>4, 2% C), La (pH>4.5, 1% C), as well as Ni and Zn (both pH>5) with increasing pH and C (Figure 4d-g). No clear trends were found for Cd, Cu, Co, Cr, Mn, and Pb.

Besides inundation with SW, the estuary system is prone to flooding with BW when SW and RW are mixing (Basallote et al., 2019). To examine the influence of salinity and pH on metal(loid) mobilization, upper layers of all cores were incubated with three types of BW (20% SW: pH 4.3 & 4.5, 12 mS/cm; 50% SW: pH 4.9 & 5.7, 28 mS/cm; 80% SW: pH 6.5 & 7.0, 42 mS/cm, for Río Odiel und Río Tinto, respectively). Metal(loid) mobilization increased with increasing SW contribution (increasing ionic strength & pH) in all cores for most elements, e.g. Cu (Figure 4i), except for Fe, As, and V (Figure 4h, A12). Brackish water with 20-50% SW contribution showed the potential to partially sequester contaminants transported by RW especially for Al, Cd, Cr, La, Ni, Pb, U, and Zn (Figure 4i & k, negative values compared to BW blanks indicate sequestration to the sediment). The pore-water pH was independent from ionic strength and pH of incubation water and solely determined by the sediment pH (Figure A13). However, cores with sediment pH above incubation water pH (TB, TC, OA, and OB) showed increased pore-water pH after flooding and enhanced sorption of cations e.g. Al, Ni, and Zn.

After the first general characterization, sediment cores TA1 and TB were used for more detailed experiments on metal(loid) mobilization as those cores were representing two common sediment types in the estuary. Tinto A1 was characterized by acidic sediment pH, low C content, and high cation mobilization whereas TB had a more alkaline sediment pH, high C content, and high As mobilization.

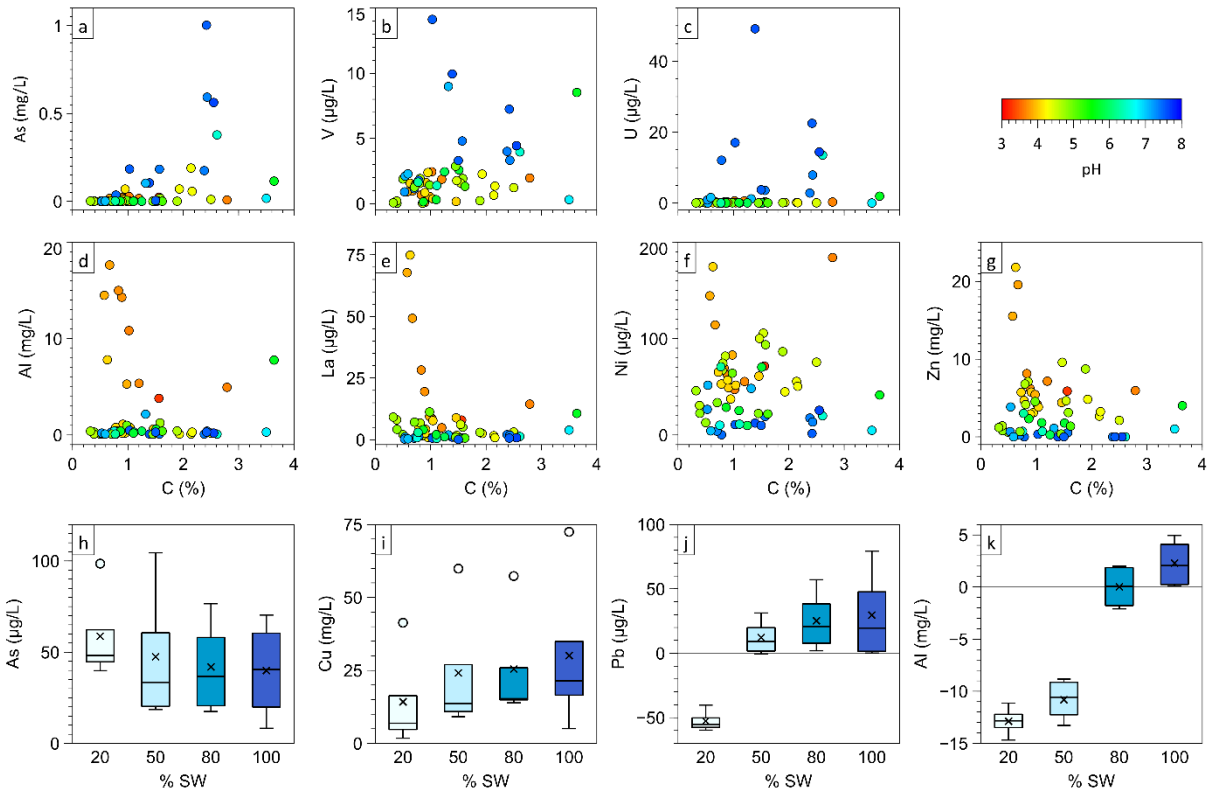

Figure 4a-g: Potential mobilization for selected metal(loid)s after 65 d SW incubation in individual core layers against carbon content (%). SW pH after incubation is shown by color. Data for all elements are shown in Figure A9 and A10. 4h-k: Potential metal(loid) mobilization (positive values) or sequestration (negative values) of upper layers at TA1 after incubation with BW and SW (20% SW: pH 4.5, 12 mS/cm; 50% SW: pH 5.7, 28 mS/cm; 80% SW: pH 7, 42 mS/cm, Río Tinto). Box plots: line, median; cross, mean; box, interquartile range; whiskers, 1.5 interquartile range; circle: outlier. Data for all elements and cores are shown in Figure A12.

3.3 Enhancing short-term metal(loid) mobilization upon SW inundation

For results more comparable to natural conditions, sediments for short-term experiments were not dried prior to inundation with RW, BW and SW and inundation was performed with 200 g of sediment to avoid depletion of nutrients or accumulation of reaction products. Monitoring metal(loid) mobilization over 60 d, an initial mobilization pulse was seen in TA1 for all elements except Fe, As, and Se on day 1 that decreased to stable concentrations until day 10 (Figure A14, A15). The effect was less pronounced in TB as cation mobilization was lower in this sediment.

After sediments reached equilibrium, two main driving factors for metal(loid) mobilization were observed: pH and salinity (conductivity). Cations, except Fe, showed higher mobilization with more acidic pore-water pH in TA1 (orange points) than under more alkaline conditions in TB (blue points) (Figure 5c-f, h-k, n & o, A16), whereas anions As and Se showed the opposite behavior with higher mobilization under alkaline pH (Figure 5b & g) with increasing SW concentration.

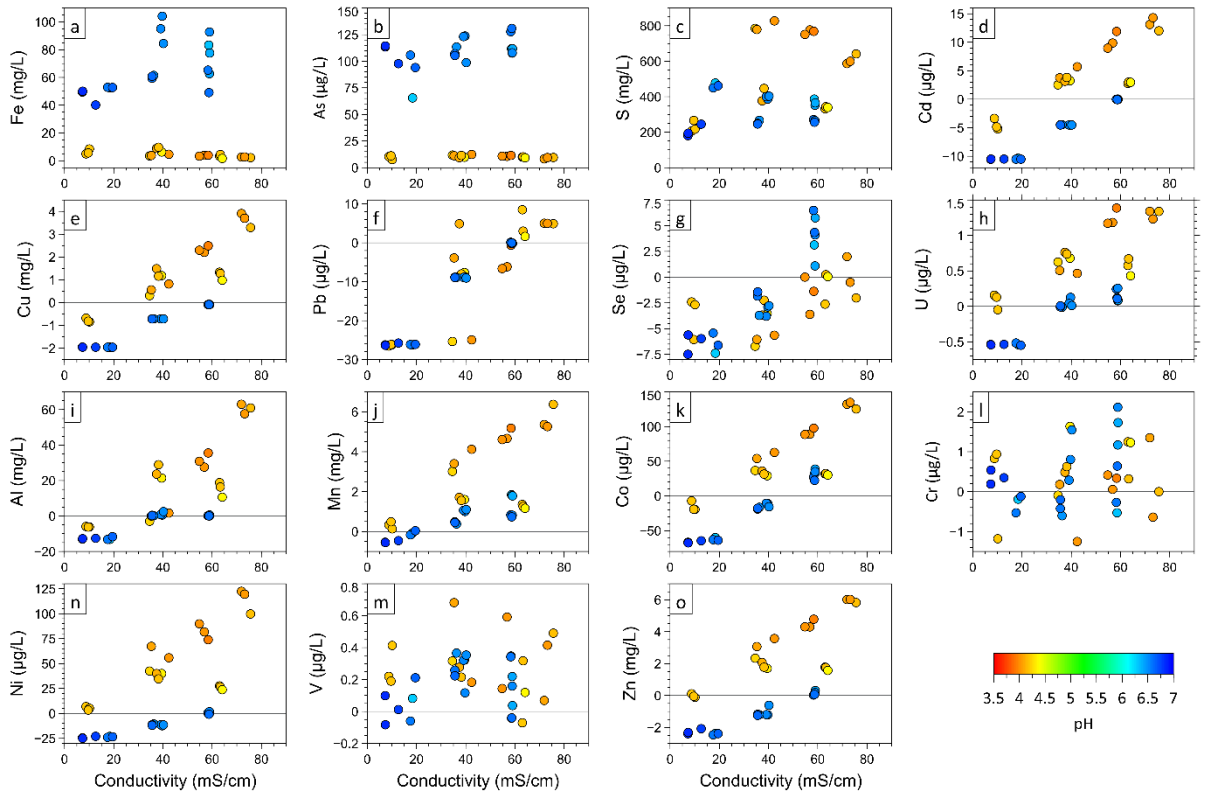

Figure 5: Short-term metal(loid) mobilization of TA1 (orange points) and TB (blue points) in bulk sediment flooded with RW, BW or SW for 60 d under stagnant conditions. Conductivity and pH were measured after 60 d in pore-water. Negative values show immobilization of metal(loids) compared to inundation water.

To investigate whether influence of waves and sediment disturbance could cause the initial pulse mobilization in the inundation experiments, shaking experiments with different solid:solution ratios (SSR) were performed. Mobilization was increased for nearly all elements in samples with shaking compared to those without shaking at similar SSRs (Figure A17) which shows that physical sediment disturbance can lead to additional mobilization. However, further increased mobilization with higher SSR was mainly seen for TB and no difference or rather a decrease in mobilization was seen for TA1. While no differences in amorphous Fe phases were found between TA1 and TB (Table A3; 45 & 42 g/kg, respectively), sequential extraction of the original sediments (Appendix D) showed that more metal(loid)s are stored in the labile fraction in TB, e.g. 0.76±0.03 µg/kg As versus 0.12±0.00 µg/kg As in TA1 (same for Cd, Pb, Co, Ni, U, Zn; less pronounced for Mn, Se) and were released by competitive desorption. Comparing the results to the initial pulse mobilization seen within the first 10 d of SW inundation in TA1 (Figure A14 & A15), the high mobilization of TB seems counterintuitive at first glance. However, high SSR increased the pore-water pH compared to inundations (Fig. 5) and with that hindered cation mobilization in TA1.

In order to test the influence of labile C input after extreme events, TA1 sediment was amended with 0-1% glucose and inundated with SW for 60 d. Addition of 0.1 and 1% glucose decreased pe+pH values compared to the control (10.9±0.1 compared to 13.0±0.3) and clearly mobilized Fe and anions As, Sb, and V sorbed to Fe-minerals (Figure 6a,b,d & f, A18, A19). A lower increase in mobilization was seen for Se (Figure 5e). High C input additionally increased Cu mobilization (Figure 5c). The labile C input did not hinder cation mobilization compared to the control without C. Interestingly, the susceptibility of small pH changes can be seen when comparing the control inundations from this experiment to the experiment done in 2021. The bulk sediment had a slightly higher pH in 2022 (4.7) compared to 2021 (4.0) and an immediately decreased cation mobilization, e.g. for Al, could be observed (Figure A14 & A19).

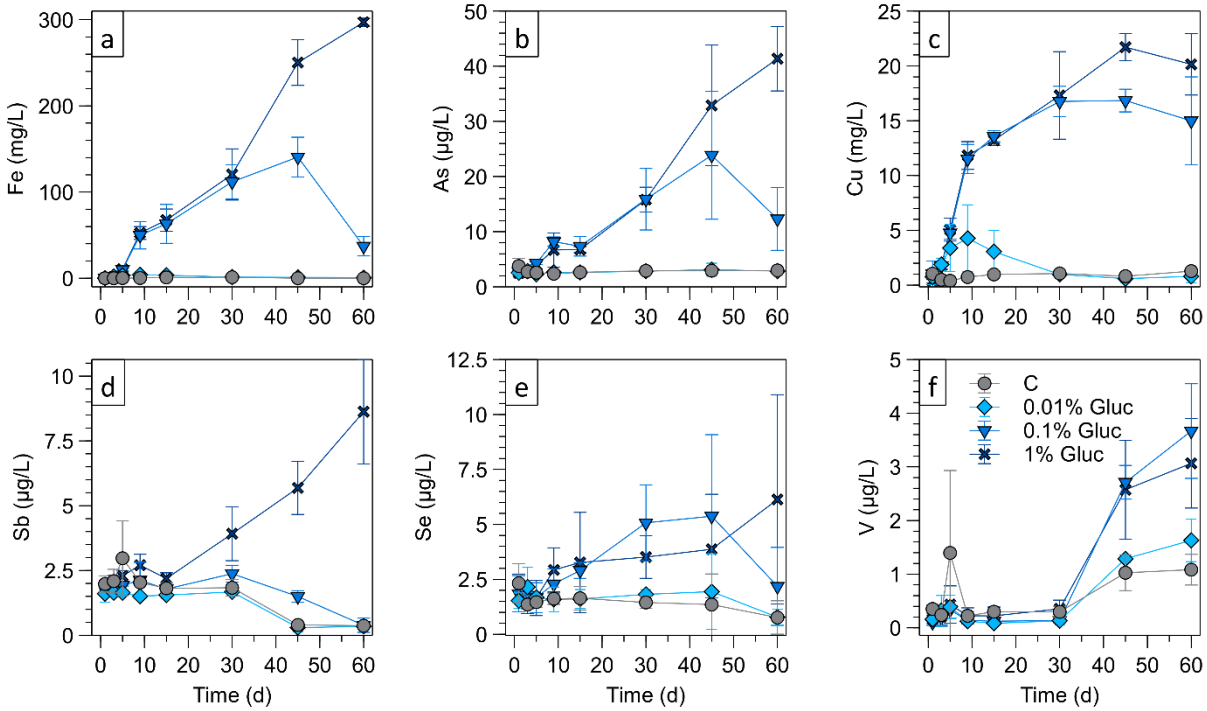

Figure 6: Short-term metal(loid) mobilization of TA1 after C-addition of 0, 0.01, 0.1, 1% C as glucose and SW flooding. Data shown for elements where mobilization was enhanced upon C addition. Data for all elements are shown in Figure A18.

3.4 Long-term metal(loid) mobilization from sediment cores under stagnant and tidal SW inundation

While incubation experiments can serve as a proxy for potential metal(loid) mobilization, long-term inundation of intact cores will show current mobilization of the undisturbed natural system. Within 1 a of SW inundation, sediment pH in TA1 upper layers became more alkaline (pH 4.9 to 6.0) and the pH increase was clearly enhanced under tidal flooding (pH 6.7, Figure 7a). However, no large changes were seen for TB as the sediment pH was already alkaline (pH 7.1). Contrasting trends were also seen for transformation of Fe mineral phases. Site TA1 showed little differences between stagnant and tidal

inundation. Upper layers were initially dominated by crystalline Fe-phases (45% and 30% amorphous Fe in stagnant and tidal cores) that transformed to more amorphous phases within 100 d (33-44% and 21% crystalline Fe) and re-crystallized within 1 a (52% and 12% amorphous Fe; Figure 7b, A20). Tidal inundation of TB showed similar trends compared to TA1, while crystalline Fe phases were completely depleted after 1 a in the stagnant TB and only amorphous Fe was available (61±12 g/kg). Total Fe concentrations were constant (around 110 and 80 g/kg in TA1 and TB) over time and changes in Fe phases cannot be attributed to Fe loss. Contaminant reservoirs in the Tinto estuary are so high that even after 1 a of tidal or stagnant inundation no obvious changes were found in the total metal(loid) content of cores (Figure A21).

Measured redox potential in the overlaying water indicates that reducing conditions were only established in stagnant TB core (pe+pH 8, Table A9) while stagnant core TA1 stayed suboxic (pe+pH 11). Hence, reductive Fe dissolution was highest under stagnant conditions at TB dissolving crystalline Fe and re-precipitating amorphous Fe phases. Limited in labile C, reactive Fe dissolution was low in TA1 and the cores reached a steady-state equilibrium within 1 a. Both tidal systems had slightly suboxic to oxic conditions (pe+pH 13 & 14) which was in line with little Fe transformation observed. Compared to SW inundations, lower metal(loid) contents were mobilized in both stagnant cores (0.01-53 % and 0.01-73% less for TA1 and TB, respectively). More mobilization was seen for Mn with 114% in TA1 and As (251%) and U (196%) in TB. Metal(loid) mobilization in TA1, even though lower than in SW inundations, was still above environmental quality standards (Table A8) for Cd (10 µg/L), Cu (29 mg/L), Ni (29 µg/L), and Zn (1.9 mg/L), however As mobilization (3.6 µg/L) was very little with As concentrations even below drinking water guidelines. The situation at site TB is exactly opposite to TA1 since environmental quality standards were met for all elements, except for As (290 µg/L). Low mobilization of metal(loids) at TB is most likely due to sorption to newly formed amorphous Fe phases as the pH of overlying water is rather similar at both sites (6.0 at TA1 and 7.1 at TB).

Tidal inundation showed high initial mobilization pulses for Mn, Cu, and Zn especially in TA1 after 24 d into the 10 L SW reservoir (Table A9). Lower concentrations measured thereafter could result from immobilization of contaminants into the sediment, however, several leakages in the experimental setup required refilling with fresh SW, also lowering the contaminant load. One factor that our inundation setup could not mimic was wave moment that was found to contribute to mobilization in separate experiments as described before.

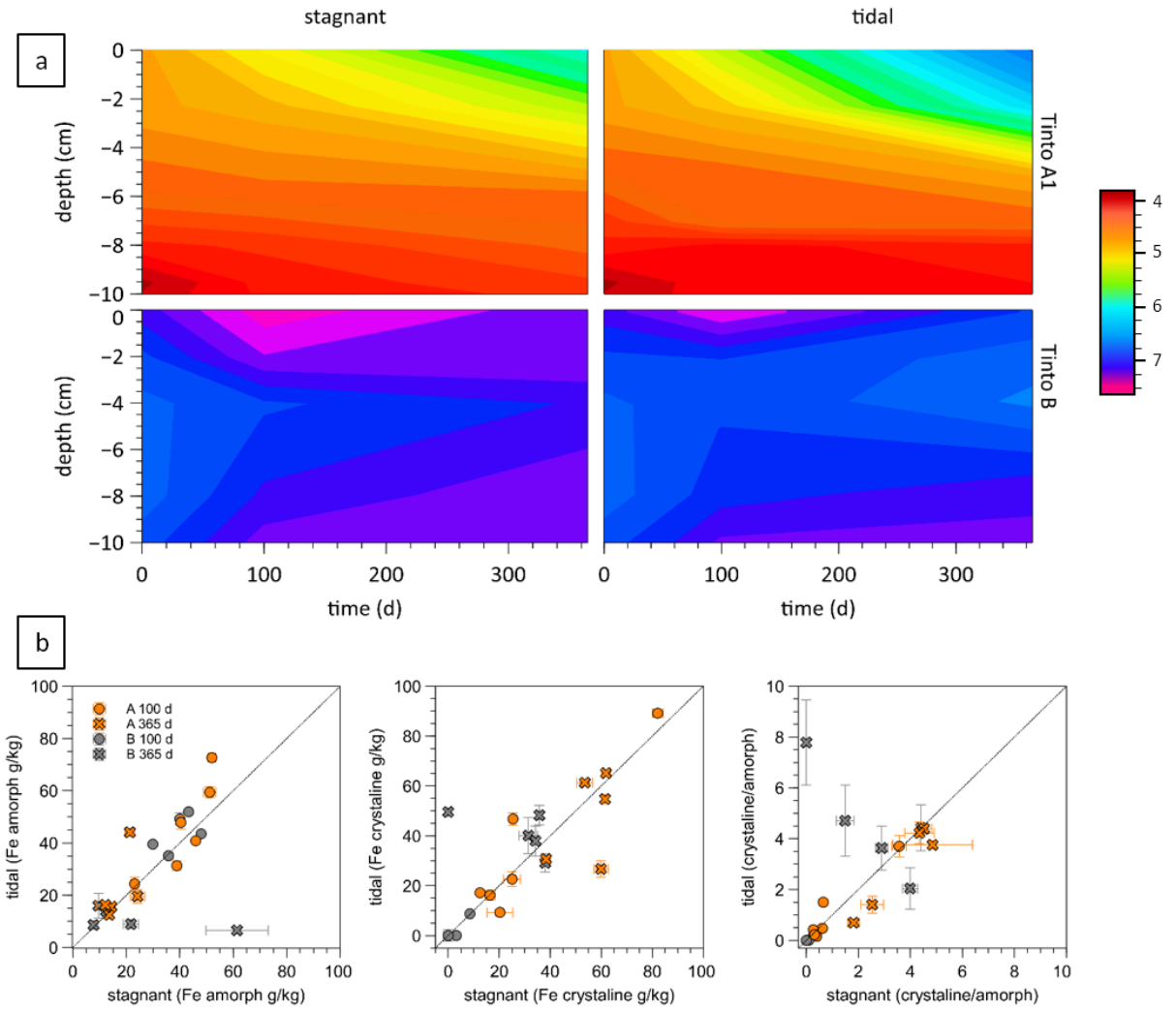

Figure 7a: pH changes over 1 a during long-term tidal and stagnant SW inundation. Sediment pH after inundation is shown by color b: Amorphous and crystalline Fe phases and their ratio comparing stagnant and tidal inundation. Cores were sampled after 0, 100, and 365 d.

3.5 Future implication of sea level rise for estuaries polluted with metal(loids)

Predicted flooding of the Ría of Huelva estuary under future climate conditions will severely influence the metal(loid) loads stored in the sediments and pose the risk to re-mobilize currently sequestered contaminants. Independent of sediment chemistry, physical disturbance, e.g. tide or waves (Figure A17), will break down sediment aggregates or weather mineral surfaces (Morales et al., 2019) and thus release sorbed ions or smaller particles with a larger surface area enhancing metal(loid) mobilization by competitive desorption from before non-accessible sorption sites.

One main chemical driving factor for metal(loid) mobilization was the sediment pH. Cations showed higher mobilization with more acidic pore-water pH (e.g. in TA1) than under more alkaline conditions (e.g. in TB) (Figure 4 & 5), whereas the anions As and Se showed the opposite behavior with higher

mobilization under alkaline pH. Under acidic sediment conditions, more surface sites are positively charged due to highly protonated functional groups favoring desorption of cations in the order of their first hydrolysis constant (Cr^{3+}<Al^{3+}<Cu^{2+}~Pb^{2+}<Zn^{2+}<Co^{2+}~Ni^{2+}<Cd^{2+}<Mn^{2+}) (Blume et al., 2016; Forbes et al., 1976). At alkaline conditions, sediment surfaces are negatively charged due to more deprotonated functional groups and anion desorption decreases according to their pK_{a1}. Pore-water pH was independent from the ionic strength of inundation water and solely determined by the sediment pH (Figure A13) as observed before (Blume et al., 2016; Wong et al., 2010). Interestingly, low sediment pH (3.8-6.4) led to even further decreased pore-water pH (3.2-5.9) after flooding with SW (pH 8.2), while higher sediment pH (5.0-7.4) led to increased pore-water pH (5.6-7.7). Competitive desorption leads to additional proton mobilization and hydrolysis of released cations additionally increases proton concentrations (Wong et al., 2010; Wright et al., 1988). However, this effect is not observed in the same intensity for all sediments especially not for TA1 and reasons for this remained unclear.

The second factor greatly influencing mobilization was ionic strength (salinity) leading to higher mobilization with higher ionic strength independent of pH (Figure 5, A16). Similar trends were seen when single layers of all cores were incubated anoxically with BW and SW (Figure 4, A9) or for inundated costal sediments (Wong et al., 2015). High ionic strength increases competitive cation desorption by introducing high concentrations of Na^{+}, Mg^{2+}, and Ca^{2+} to the system (Wright et al., 1988). At low ionic strength, initial sediment pH is the main driver for metalloid mobilization or sequestration, however, with increasing ionic strength competitive desorption overrules pH influences and acts as the main driver for metal(loid) mobilization. High ionic strength did not increase As and Fe mobilization in TA1 due to low reductive dissolution of Fe caused by labile C limitation of site TA1 (see 3.3). Arsenic was mainly bound to amorphous and crystalline Fe-/Mn-oxides at this site (Table A10, Appendix D) and therefore not desorbed by solely increasing ionic strength.

Under predicted climate change scenarios, extreme events such as floods, storms, or droughts are more likely (IPCC, 2021) and those events could release labile C to the estuary system by e.g. overflowing wastewater treatment plants, oil or manure spills, or producing dead biomass from seasonal algae blooms (Cramer et al., 2018; Lange, 2020). Currently, sediment TA1 has lower sediment C (Table A3) than TB and all experiments showed that Fe-minerals in TA1 were fairly stable, even under long-term stagnant inundation as the redox potential remained suboxic not reaching anoxic conditions (Figure A18, Table A9). These observations hint towards low availability of labile C in the sediment hindering microbially mediated reductive Fe dissolution. However, if future climate extreme events increase labile C availability, Fe and the anions As, Sb, and V will be mobilized (Figure 6, A19) as observed before for As (LeMonte et al., 2017). Besides anions, more Cu was mobilized due to its high affinity to C. High DOC concentrations in the pore-water will mobilize Cu by formation of Cu-DOC complexes (Mehlhorn et al., 2018). The labile C input did not hinder cation mobilization compared to

the control without C, so labile C input turned TA1 sediment into both a source for cation as well as anion leaching.

Taking the factors into account that will influence metal(loid) mobilization under future climate conditions, the following short- and long-term scenarios are predicted. In the near future, the estuary will be sporadically flooded with BW after extreme events e.g. storms or heavy rain and metal(loid) mobilization will be governed by sediment pH and the salinity of the BW. Especially acidic sediments will be prone to cation mobilization if the BW contains more than 50% SW (Figure 4, 5). Larger inputs of labile C during these extreme events pose an additional risk in currently C-limited acidic sediments. These sediments have a naturally high cation mobilization that is not hindered by additional C, however, enhanced reductive dissolution of Fe-minerals will also mobilize currently sequestered anions (Figure 6).

Over several decades with elevated sea levels, larger parts of the estuary will be permanently inundated with SW. Considering the results from the 1 year-SW inundation, the most likely scenario is that acidic sediments flooded with SW will reach rather neutral sediment pH over time (Figure7). The higher pH will decrease cation mobility compared to previous acidic conditions and as suggested from our results might limit net mobilization of Cd, Cu, Pb, Al, Ni, Zn (Figure 5) similar to observations under different hydrological regimes in the estuary (Basallote et al., 2019). Even though SW inundation might limit net mobilization, measured pore-water concentration for potentially toxic elements, e.g. Zn (Figure A16) were still above environmental quality standards (BOE, 2015) and more cations could easily be liberated into SW by waves and sediment disturbance. Further, anion mobilization will remain problematic under neutral to alkaline sediments pH as seen in TB (Figure 5) and As pore-water concentrations also were found to be above environmental quality standards (BOE, 2015).

5 Conclusion

Under current climatic conditions, the Ría of Huelva is a highly contaminated estuary system with a strongly increasing pH gradient towards the coast and high spatial heterogeneity in metal(loid) load. Current contaminant loads in the sediments exceed action limits in an increasing order for Cd, Zn, Pb, Cu, and As. Potential metal(loid) mobilization under predicted SW and BW flooding led to further exceeding of water quality standards in increasing order for As, Pb, and Zn~Ni~Cu~Cd. While solely sediment loads could not be used to predict mobilization, sediment pH and salinity were identified as the main driving factors. Cation and anion mobility were found to be mainly pH-controlled under low salinity, while competitive desorption overruled pH effects with increasing SW content. In sediments limited in labile C, input of labile C enhanced reductive Fe dissolution causing mobilization of anions or C-associated elements, e.g. Cu. Independent from sediment chemistry, physical disturbances as waves

or strong floods contributed to metal(loid) mobilization by breakdown of sediment aggregates and minerals.

Rising sea level will first affect already alkaline sediments closer to the coast like site TB and enhance currently low cation mobilization mainly by increasing salinity, while high anion mobilization due to reductive Fe dissolution will remain. Highest contaminant mobilization can be expected once acidic sediments further inland that have a high contaminant load (TA1) will be flooded with SW. On the short-term, high ionic strength will further increase cation mobilization as sediment pH is still acidic. On long-term scenarios, sediment pH will be neutralized by SW and thus limit cation mobilization to levels observed at site TB. Considering long-term scenarios for the Ría of Huelva estuary is important, as the contaminant load in the sediment is so high that slow mobilization to the SW could last for more than 1000 years, e.g. for As, Pb, and Al (linearly extrapolating mean potential mobilization in the estuary). The results obtained in this study could be useful to predict short- and long-term scenarios of metal(loid) release upon climate change in other estuaries worldwide affected by metal(loid) pollution.

Notes

The authors declare no competing financial interest.

Acknowledgement

We thank Sylvia Hafner and Stefan Will for help with ICP-MS measurements and Milagros Galaraza Nuñez for keeping the tidal flooding pumps working. This work has largely been funded by seed money from the University of Bayreuth, Germany. M.D.B. thanks the Spanish Ministry of Science and Innovation for the Postdoctoral Fellowship (IJC2018-035056-I). Field work has been partially supported by the Consejería de Transformación Económica, Industria, Conocimiento y Universidades from Andalusian Government through the Andalusian FEDER operational program 2014–2020 (FEDER UHU2020-21 Project) and the Spanish Ministry of Economy and Competitiveness under the research project TRAMPA (MINECO; PID2020-119196RB-C21). C.R.C thanks the Spanish Ministry of Science and Innovation for the Postdoctoral Fellowship (RYC2019-027949-I).

6 References

Achterberg EP, Herzl VM, Braungardt CB, Millward GE. Metal behaviour in an estuary polluted by acid mine drainage: the role of particulate matter. Environ Pollut 2003; 121: 283-92.

Allen HE. The significance of trace metal speciation for water, sediment and soil quality criteria and standards. Science of the total environment 1993; 134: 23-45.

Asta MP, Calleja ML, Pérez-López R, Auqué LF. Major hydrogeochemical processes in an Acid Mine Drainage affected estuary. Marine pollution bulletin 2015; 91: 295-305.

ASTM. Standard Practice for the Preparation of Substitute Ocean Water. D 1141. ASTM International, West Conshohocken, PA, United States, 2003.

Atkinson CA, Jolley DF, Simpson SL. Effect of overlying water pH, dissolved oxygen, salinity and sediment disturbances on metal release and sequestration from metal contaminated marine sediments. Chemosphere 2007; 69: 1428-1437.
Bamber JL, Oppenheimer M, Kopp RE, Aspinall WP, Cooke RM. Ice sheet contributions to future sea-level rise from structured expert judgment. Proceedings of the National Academy of Sciences 2019; 116: 11195-11200.
Basallote MD, Cánovas CR, Pérez-López R, Olías M, Macías F, Nieto JM. Metal partitioning and pH-buffering during mixing processes in an estuary strongly affected by acid mine drainage–The Ria de Huelva estuary (SW Spain). 2019.
Benach J, Yasui Y, Martínez JM, Borrell C, Pasarin M, Daponte A. The geography of the highest mortality areas in Spain: a striking cluster in the southwestern region of the country. Occupational and Environmental Medicine 2004; 61: 280-281.
Blume H-P, Brümmer GW, Fleige H, Horn R, Kandeler E, Kögel-Knabner I, et al. Chemical Properties and Processes. Scheffer/SchachtschabelSoil Science. Springer Berlin Heidelberg, Berlin, Heidelberg, 2016, pp. 123-174.
BOE. Real Decreto 817/2015, de 11 de septiembre, por el que se establecen los criterios de seguimiento y evaluación del estado de las aguas superficiales y las normas de calidad ambiental. In: Ministerio de Agricultura AyMA, editor. BOE-A-2015-9806, 2015, pp. 96.
Borrego J, Morales J, De la Torre M, Grande J. Geochemical characteristics of heavy metal pollution in surface sediments of the Tinto and Odiel river estuary (southwestern Spain). Environmental Geology 2002; 41: 785-796.
Canovas CR, Basallote MD, Macias F. Distribution and availability of rare earth elements and trace elements in the estuarine waters of the Ria of Huelva (SW Spain). Environ Pollut 2020; 267: 115506.
Climatecentral.org. Costal risk screening tool. 2022. climatecentral.org, 2021.
Cline JD. Spectrophotometric determination of hydrogen sulfide in natural waters 1. Limnology and Oceanography 1969; 14: 454-458.
Cramer W, Guiot J, Fader M, Garrabou J, Gattuso J-P, Iglesias A, et al. Climate change and interconnected risks to sustainable development in the Mediterranean. Nature Climate Change 2018; 8: 972-980.
Dafner EV, Sempere R, González N, Gomez F, Goutx M. Cross-slope variations of dissolved organic carbon in the Gulf of Cadiz, NE Atlantic Ocean (February 1998). Marine Ecology Progress Series 1999; 189: 301-306.
Davis Jr R, Welty A, Borrego J, Morales J, Pendon J, Ryan JG. Rio Tinto estuary (Spain): 5000 years of pollution. Environmental Geology 2000; 39: 1107-1116.
DelValls T, Andres A, Belzunce M, Buceta J, Casado-Martinez M, Castro R, et al. Chemical and ecotoxicological guidelines for managing disposal of dredged material. TrAC Trends in Analytical Chemistry 2004; 23: 819-828.
Dold B, Diaby N, Spangenberg JE. Remediation of a marine shore tailings deposit and the importance of water-rock interaction on element cycling in the coastal aquifer. Environ Sci Technol 2011; 45: 4876-83.
Elbaz-Poulichet F, Braungardt C, Achterberg E, Morley N, Cossa D, Beckers J-M, et al. Metal biogeochemistry in the Tinto–Odiel rivers (Southern Spain) and in the Gulf of Cadiz: a synthesis of the results of TOROS project. Continental Shelf Research 2001; 21: 1961-1973.
Fiedler S, Vepraskas MJ, Richardson JL. Soil Redox Potential: Importance, Field Measurements, and Observations. 2007; 94: 1-54.
Fischer L, Brümmer G, Barrow N. Observations and modelling of the reactions of 10 metals with goethite: adsorption and diffusion processes. European Journal of Soil Science 2007; 58: 1304-1315.
Forbes E, Posner A, Quirk J. The specific adsorption of divalent Cd, Co, Cu, Pb, and Zn on goethite. Journal of soil science 1976; 27: 154-166.
Gaonkar CV, Matta VM. Impact of mining on metal concentration in waters of the Zuari estuary, India. Environ Monit Assess 2019; 191: 368.
Han Y-S, Park J-H, Kim S-J, Jeong HY, Ahn JS. Redox transformation of soil minerals and arsenic in arsenic-contaminated soil under cycling redox conditions. Journal of hazardous materials 2019; 378: 120745.
Hutchings AM, Antler G, Wilkening JV, Basu A, Bradbury HJ, Clegg JA, et al. Creek Dynamics Determine Pond Subsurface Geochemical Heterogeneity in East Anglian (UK) Salt Marshes. Frontiers in Earth Science 2019; 7.
IPCC. The Physical Science Basis. Contribution of Working Group I to the Sixth Assessment Report of the Intergovernmental Panel on Climate Change. In: Masson-Delmotte V, P. Zhai, A. Pirani, S.L. Connors, C. Péan, S. Berger, N. Caud, Y. Chen, L. Goldfarb, M.I. Gomis, M. Huang, K. Leitzell, E. Lonnoy, J.B.R. Matthews, T.K. Maycock, T. Waterfield, O. Yelekçi, R. Yu, and B. Zhou editor. Climate Change 2021. Cambridge University Press, Cambridge, United Kingdom and New York, NY, USA, 2021.

Johnston SG, Keene AF, Burton ED, Bush RT, Sullivan LA, McElnea AE, et al. Arsenic mobilization in a seawater inundated acid sulfate soil. Environmental science & technology 2010; 44: 1968-1973.
Koehnken L. Macquarie Harbour-King River study. Department of Environment and Land Management; Hydro Electric Commission; The Mount Lyell Mining and Railway Company Ltd; Inland Fisheries Commission; Department of Primary Industry and Fisheries - Sea Fisheries Division; Department of Community and Health Services, 1996.
Kulp SA, Strauss BH. New elevation data triple estimates of global vulnerability to sea-level rise and coastal flooding. Nature communications 2019; 10: 1-12.
Lange MA. Climate change in the Mediterranean: environmental impacts and extreme events. IEMed: Mediterranean Yearbook 2020: 30-45.
LeMonte JJ, Stuckey JW, Sanchez JZ, Tappero R, Rinklebe Jr, Sparks DL. Sea level rise induced arsenic release from historically contaminated coastal soils. Environmental Science & Technology 2017; 51: 5913-5922.
Long ER, MacDonald DD, Smith SL, Calder FD. Incidence of adverse biological effects within ranges of chemical concentrations in marine and estuarine sediments. Environmental management 1995; 19: 81-97.
Mehlhorn J, Besold J, Lezama Pacheco JS, Gustafsson JP, Kretzschmar R, Planer-Friedrich B. Copper Mobilization and Immobilization along an Organic Matter and Redox Gradient-Insights from a Mofette Site. Environ Sci Technol 2018; 52: 13698-13707.
Mehra O. Ion oxide removal from soils and clays by a dithionite-citrate system buffered with sodium bicarbonate in Clays and Clay Minerals. Proc. 7th Natl. Conf., Washing-ton, DC, 1958. Pergamon Press, 1960.
Morales JA, Rodríguez-Ramírez A, Sedrati M. Beaches of Huelva. 2019: 335-359.
Morillo J, Usero J, Rojas R. Fractionation of metals and As in sediments from a biosphere reserve (Odiel salt marshes) affected by acidic mine drainage. Environ Monit Assess 2008; 139: 329-37.
Nieto JM, Sarmiento AM, Olias M, Canovas CR, Riba I, Kalman J, et al. Acid mine drainage pollution in the Tinto and Odiel rivers (Iberian Pyrite Belt, SW Spain) and bioavailability of the transported metals to the Huelva Estuary. Environ Int 2007; 33: 445-55.
O'Connor KP, Montgomery M, Rosales RA, Whiteman KK, Kim CS. Wetting/drying cycles increase arsenic bioaccessibility in mine-impacted sediments. Science of the Total Environment 2021; 774: 145420.
Olías M, Cánovas CR, Nieto J, Sarmiento AM. Evaluation of the dissolved contaminant load transported by the Tinto and Odiel rivers (South West Spain). Applied Geochemistry 2006; 21: 1733-1749.
Olías M, Nieto JM. Background conditions and mining pollution throughout history in the Río Tinto (SW Spain). Environments 2015; 2: 295-316.
Pérez-López R, Castillo J, Sarmiento AM, Nieto JM. Assessment of phosphogypsum impact on the salt-marshes of the Tinto river (SW Spain): Role of natural attenuation processes. Marine pollution bulletin 2011; 62: 2787-2796.
Pirrie D, Power MR, Rollinson G, Camm GS, Hughes SH, Butcher AR, et al. The spatial distribution and source of arsenic, copper, tin and zinc within the surface sediments of the Fal Estuary, Cornwall, UK. Sedimentology 2003; 50: 579-595.
Rosado D, Usero J, Morillo J. Assessment of heavy metals bioavailability and toxicity toward Vibrio fischeri in sediment of the Huelva estuary. Chemosphere 2016; 153: 10-17.
Stookey LL. Ferrozine---a new spectrophotometric reagent for iron. Analytical chemistry 1970; 42: 779-781.
Wong VN, Johnston SG, Burton ED, Bush RT, Sullivan LA, Slavich PG. Seawater causes rapid trace metal mobilisation in coastal lowland acid sulfate soils: Implications of sea level rise for water quality. Geoderma 2010; 160: 252-263.
Wong VN, Johnston SG, Burton ED, Hirst P, Sullivan LA, Bush RT, et al. Seawater inundation of coastal floodplain sediments: short-term changes in surface water and sediment geochemistry. Chemical Geology 2015; 398: 32-45.
Wright R, Norton S, Brakke D, Frogner T. Experimental verification of episodic acidification of freshwaters by sea salts. Nature 1988; 334: 422-424.